Experimental investigation of the phase relations in the SiO_2-Dy_2O_3-CaO ternary system

Fei Wang[1,2], Wenke Zhi[1], Annelies Malfliet[2*], Bin Yang[1], Bart Blanpain[2], Muxing Guo[2]

1. State Key Laboratory of Complex Nonferrous Metal Resources Clear Utilization in Yunnan Province, National Engineering Laboratory for Vacuum Metallurgy, Faculty of Metallurgical and Energy Engineering, Kunming University of Science and Technology, 650093 Kunming, People's Republic of China

2. Department of Materials Engineering, KU Leuven, Kasteelpark Arenberg 44 bus 2450, 3001 Leuven, Belgium

*Corresponding author: Annelies Malfliet, annelies.malfliet@kuleuven.be

Abstract

This paper reports on the experimental investigation of the phase relations in the CaO-SiO_2-Dy_2O_3 system. CaO-SiO_2-Dy_2O_3 slags were equilibrated at 1773 and 1873 K for 24 h in Ar and then quenched in water to determine the phase relations of the system. The composition of the equilibrated phases was measured by EPMA-WDS. The presence of ternary compounds and the extension of the solid solution and liquid regions were determined to construct the isothermal sections at 1773 and 1873 K of the ternary phase diagram. The data from this work will support further investigations on the feasibility to recover REEs through pyrometallurgical processing.

Keywords: Rare earth recovery; phase relation;; CaO-SiO_2-Dy_2O_3 system

1 Introduction

The rare earth elements (REEs) are increasingly valuable because of their growing

use in renewable energy and high technology applications [1], such as fuel cells, magnets, superconductors, cell phones, turbines and thermoelectric materials. The limited known exploitable deposits of REEs in the world, however, creates challenges in the supply of primary REEs [2]. Dy is a critical metal for the production of permanent magnets, lamp phosphors, rechargeable NiMH batteries, catalysts and for other applications [3,4,5]. As permanent magnets are the largest consumer of REEs, the recovery of Dy, Nd and other valuable metals from end of life magnets plays an important role in the future supply of REEs. Recycling of Dy from doped permanent magnets is considered as a part of the solution for a more green and sustainable future [6,7].

Hydrometallurgical processing is commonly used to recover rare earth metals from wastes [8,9] due to its high ability to separate elements with similar chemical and physical properties and due to the lower capital cost for operation at small scale compared to other processes [10]. However, the main disadvantages of hydrometallurgical routes are the need for large amounts of chemicals and water and the requirement of multiple processing steps [**Error! Bookmark not defined.**]. A combination with pyrometallurgy, therefore, has been considered as an alternative route with a potentially lower environmental impact and higher economic profit to overcome these drawbacks [11]. In pyrometallurgical processes, the rare earth elements are concentrated in the slag due to their high affinity to oxygen. Although phosphate-free silicates-based slags might have notable concentrations of REEs [12], the current challenge for the pyrometallurgists is to find an efficient extraction process to recover

the rare earths from these slags. In this context, fundamental understanding of the distribution of the rare earths in the slag is of great significance.

As the behavior of the REEs in the slag is governed by the thermodynamic equilibrium of the system, the thermodynamic properties of rare earth oxide-containing systems must be determined, which is necessary for developing high efficiency pyrometallurgical processes to recover the rare earths from secondary resources [13]. In this work, CaO-SiO_2-Dy_2O_3 slags were equilibrated at 1773 and 1873 K under Ar atmosphere, and then quenched in water to determine the phase relations of the system. The obtained data can be applied in the recovery of Dy from REE wastes through pyrometallurgical processing.

2 Materials and methods

Slags were prepared by mixing reagent-grade CaO (obtained by calcination of $CaCO_3$, 99.99%, Chempur), SiO_2 (99.9%, Merck Millipore) and Dy_2O_3 (99.99%, Chempur). The composition of these mixtures are shown in Tables 1 and 2 for the experiments at respectively 1773 and 1873 K. The powder mixture was put in a closed shallow-bottomed Pt-20% Rh envelope inside an Al_2O_3 crucible. This crucible was hung with a Pt-20% Rh wire in the hot zone of a vertical tube furnace with $MoSi_2$ heating elements. The mixtures were hold at respectively 1773 and 1873 K for 24 h in an argon atmosphere (with flow rate 500 cm^3/min), and then quenched in water. The set-up of the equilibrium experiments is shown in Fig.1.

The microstructure and phase composition of the quenched samples were determined

using an Electron Probe Micro Analyzer coupled with Wavelength Dispersive Spectroscopy (EPMA-WDS, JEOL JXA-8530F). Quantitative analysis using standards at an acceleration voltage of 15 kV and a probe current of 15 nA was performed. The average accuracy of the EPMA measurements on the main elements is ±1 wt.%. The slag samples were mounted in resin, grinded, polished and Pt coated before the EPMA-WDS assessment.

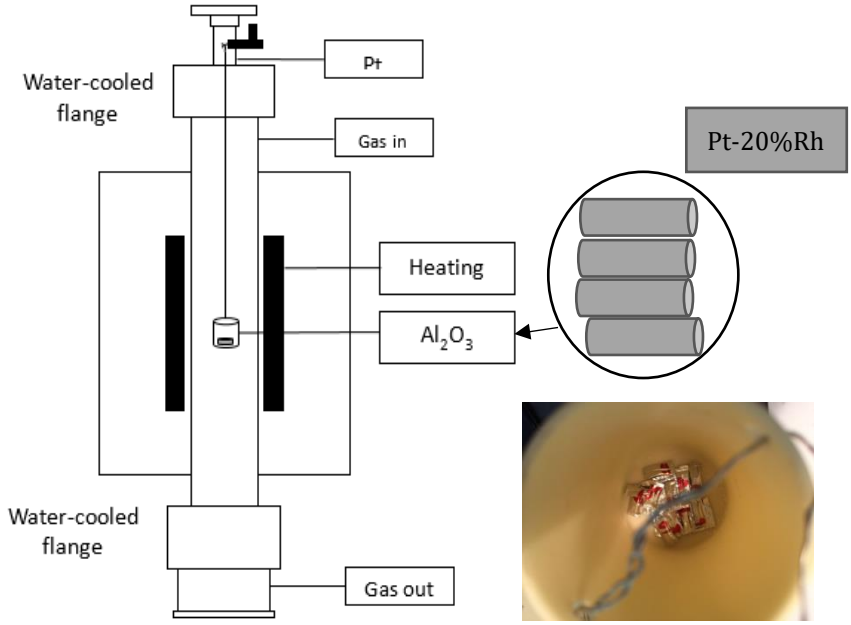

Figure 1: Schematic representation of the equilibration furnace. Multiple envelopes containing the powder mixtures with different compositions were simultaneously heated. After 24 h, the crucibles were dropped by releasing the wire from the hook, and the samples were quenched in water.

3 Literature study on the CaO-SiO_2-Dy_2O_3 system

The reported solid phases in the CaO-SiO_2-Dy_2O_3 ternary system are summarized in Table 3.

3.1Unary systems

Dy_2O_3 is stable in the cubic crystal structure below 2143 K [14,15]. At higher temperatures, it exists in the monoclinic and/or hexagonal structure. The cubic, monoclinic and hexagonal structure of Dy_2O_3 are called respectively the C-, B- and H-type. The crystal structures of CaO and SiO_2 have been widely investigated [16]. Cubic CaO (burnt lime) is stable from room temperature up to its melting temperature of 2845 K. For silica, the [SiO_4] tetrahedron is the basic structural element. At ambient conditions, trigonal α-quartz (α-SiO_2) is stable at room temperature and transforms to hexagonal β-quartz at 846 K. β-quartz converts to hexagonal β-tridymite at 1143 K and then transforms to cubic β-cristobalite at 1743 K. The melting temperature of β-cristobalite is 1978 K.

3.2 Binary systems

The CaO-SiO_2-Dy_2O_3 system consists of three binary subsystems, namely the CaO-SiO_2 [16], CaO-Dy_2O_3 [17] and SiO_2-Dy_2O_3 [18] system.

The CaO-SiO_2 system has been experimentally investigated and thermodynamically optimized by Eriksson et al. [16] and. Hillert et al. [19] The CaO-Dy_2O_3 binary phase diagram was reported by Lopato et al. [17]. It includes the two binary phases, $CaDy_2O_4$ and $CaDy_4O_7$, which are stable in the temperature range ~1810-2230 K and ~1970-2520 K respectively. Their crystal structure is similar to $CaFe_2O_4$ and $CaFe_4O_7$ [20]

respectively. CaO has an appreciable solubility in both the C-, B- and H-type structure of Dy_2O_3 [17][21]. In the Dy_2O_3-SiO_2 system, three binary compounds have been reported by Toropov et al., [18] namely Dy_2SiO_5, $Dy_2Si_2O_7$ and $Dy_4Si_3O_{12}$. The miscibility gap and the metastability in the SiO_2-Dy_2O_3 system were investigated by Kim et al.[22].

According to the above literature information of the unary and binary systems, within the temperature range of this investigation (1773-1873 K), the stable unary and binary phases are: cubic CaO, β-cristobalite SiO_2, C-type Dy_2O_3, $CaDy_2O_4$, $CaDy_4O_7$, Dy_2SiO_5, $Dy_2Si_2O_7$, Ca_3SiO_5, α-Ca_2SiO_4 and $CaSiO_3$ (only stable up to 1817 K).

3.3 Ternary system

In CaO-SiO_2-RE_2O_3 ternary systems, $(Ca,RE)_{9.33}(SiO_4)_6O_2$ (RE = ,,,) is considered to be a stable phase in which larger RE cations substitute Ca in the crystal lattice [23]. Experience in the CaO-SiO_2-RE_2O_3 system indicates that $Ca_3RE_2Si_3O_{12}$ and $Ca_3RE_2Si_6O_{18}$ should be line compounds while in apatite and cuspidine can exhibit solid solution homogeneity ranges enabled by ionic substitutions [24, 25]. The formation of these ternary compounds is considered to occur in a similar manner in the ternary CaO-SiO_2-Dy_2O_3 system due to the similarities between the lanthanides.

4 Results and discussion

The phase relations in the CaO-Dy_2O_3-SiO_2 system at 1773 and 1873 K were investigated by compositional and microstructural analysis of the equilibrated and quenched samples having at least 2 homogeneous phases in equilibrium (Figure 2). For each sample, at least 10 compositions were measured for each phase and the average value is used to determine the phase equilibria. The identified phases and their composition are summarized in Tables 4 and 5. The data are organized such that all measurements relating to a particular primary phase field or a combination of phases are grouped together.

4.1 Construction of the CaO-Dy_2O_3-SiO_2 isothermal sections at 1773 and 1873 K

From the phase equilibria, the isothermal sections at 1773 and 1873 K of the Ca_2SiO_4(C_2S)-SiO_2-Dy_2O_3 region in the CaO-SiO_2-Nd_2O_3 system were constructed by applying Rhines' ten empirical rules and the boundary theory [26] (Figure 3). The results provide mainly data about the extent of the liquid region and the two- and three-phase equilibria around the liquid region. The location of the liquidus in the binary CaO-SiO_2 was drawn in accordance with the data from the accepted binary phase diagram [19].

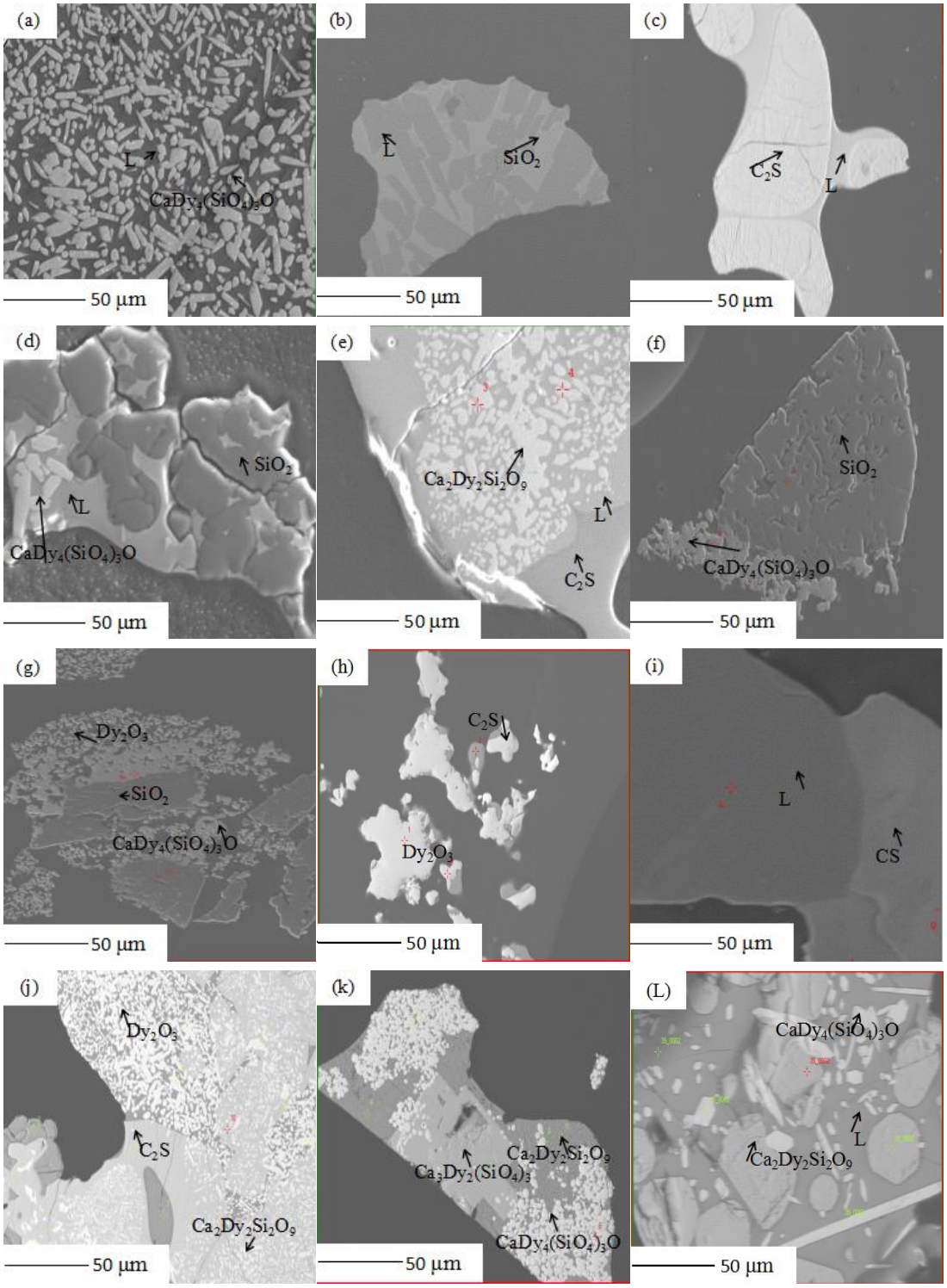
(a)
L
$CaDy_4(SiO_4)_3O$
50 µm
(b)
L
SiO_2
50 µm
(c)
C_2S
L
50 µm
(d)
SiO_2
L
$CaDy_4(SiO_4)_3O$
50 µm
(e)
$Ca_2Dy_2Si_2O_9$
L
C_2S
50 µm
(f)
SiO_2
$CaDy_4(SiO_4)_3O$
50 µm
(g)
Dy_2O_3
SiO_2
$CaDy_4(SiO_4)_3O$
50 µm
(h)
C_2S
Dy_2O_3
50 µm
(i)
L
CS
50 µm
(j)
Dy_2O_3
C_2S
$Ca_2Dy_2Si_2O_9$
50 µm
(k)
$Ca_2Dy_2Si_2O_9$
$Ca_3Dy_2(SiO_4)_3$
$CaDy_4(SiO_4)_3O$
50 µm
(L)
$CaDy_4(SiO_4)_3O$
L
$Ca_2Dy_2Si_2O_9$
50 µm

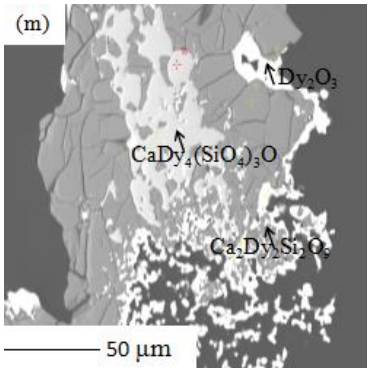

Figure 2: BSE images of the quenched CaO-SiO_2-Dy_2O_3 samples from the equilibrium experiments at 1773 and 1873 K.

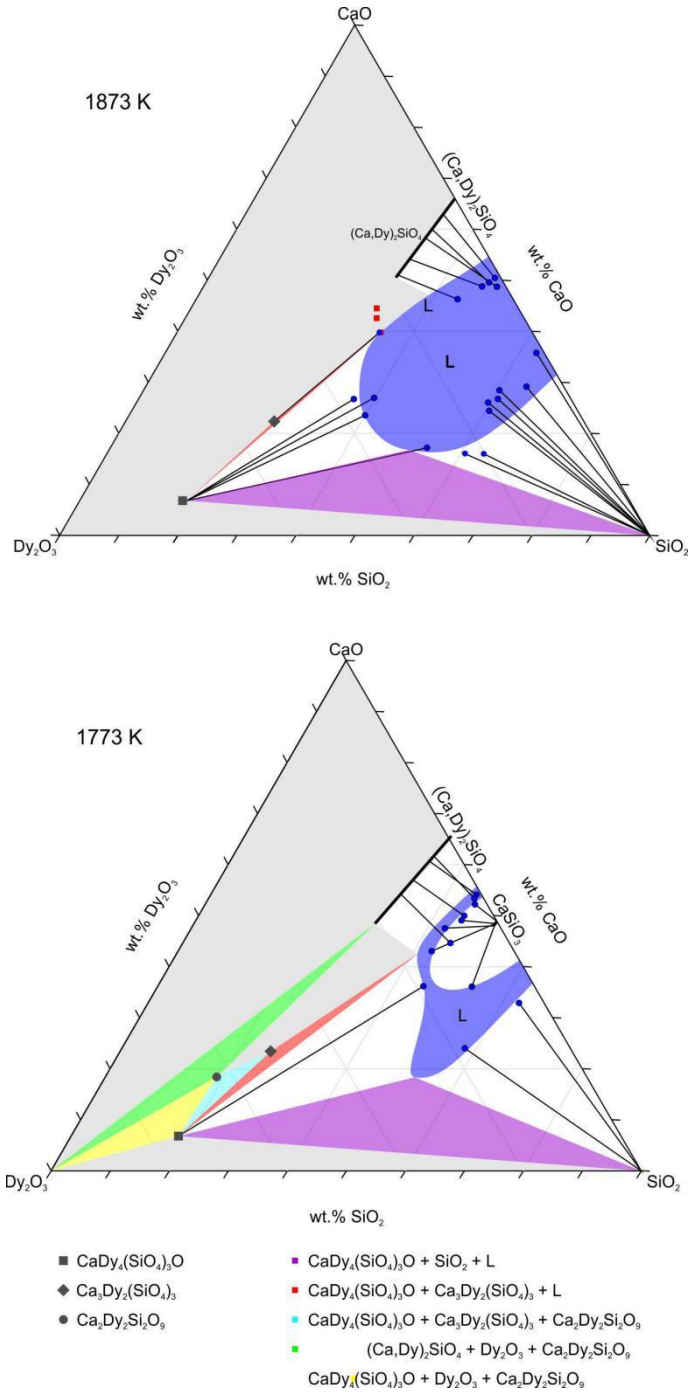

Figure 3: Experimentally established phase relations of the CaO-SiO_2-Dy_2O_3 system at 1873 and 1773 K.

4.2 Solubility of Dy_2O_3 in the binary CaO-SiO_2 phases

The maximum concentration of Dy_2O_3 dissolved in $(Ca,Dy)_2SiO_4$ in a two-phase equilibrium with the liquid was measured as 13.9 and 18.5 wt.% at 1773 and 1873 K, respectively. In equilibrium with Dy_2O_3 and $Ca_2Dy_2Si_2O_9$, $(Ca,Dy)_2SiO_4$ dissolves 20.9 wt.% Dy_2O_3 at 1773 K.

On the other hand, the solubility of Dy_2O_3 in the $CaSiO_3$ phase at 1773 K is low. A maximum concentration of 0.8 wt.% Dy_2O_3 was measured in the $CaSiO_3$ phase in equilibrium with the liquid phase.

4.3 The ternary CaO-SiO_2-Dy_2O_3 phases

The apatite phase with the general formula $Ca_xRE_{10-x}(SiO_4)_6O_{3-0.5x}$ [27] was observed at 1773 and 1873 K for x=2, giving $CaDy_4(SiO_4)_3O$. The other ternary phase observed at both temperatures has the formula $Ca_3Dy_2(SiO_4)_3$, which seems to correspond to the silico-carnotite phase reported by Piccinelli et al. [32].

4.3 The liquid region

The two-phase equilibria between liquid and $CaSiO_3$, $(Ca,Dy)_2SiO_4$, SiO_2, $CaDy_4(SiO_4)_3O$ and $Ca_3Dy_2(SiO_4)_3$ are indicated in Figure 3. These solid phases are the primary crystalline phases to form from the liquid phase upon cooling from either 1873 or 1773 K. The solubility of Dy_2O_3 in the liquid phase increases with increasing temperature, with a maximum measured concentration of 34.1 and 37.3 wt.% Dy_2O_3 at respectively 1773 and 1873 K.

4.4 Enrichment and recovery feasibility of REEs

Based on the experimentally determined phase relations in the Dy_2O_3-containing slag system, two schemes are identified to enhance the recovery of Dy_2O_3. In the first scheme, the composition of the system can be modified to be in the two-phase CS-L region at a temperature around 1773 K. Upon cooling, the Dy_2O_3-lean CS phase will precipitate, thereby concentrating Dy_2O_3 in the liquid phase. In the second scheme, the composition of the system is modified to fall within the $CaDy_4(SiO_4)_3O$-SiO_2-L region. Upon cooling, both $CaDy_4(SiO_4)_3O$ and SiO_2 will precipitate from the liquid phase. The separation between the apatite phase and the liquid phase can be achieved through their difference in density, as it was also observed in the lab-scale tests (Figure 4). The concentration of Dy_2O_3 in the apatite phase could ease and improve the REEs recovery process, thereby improving the economic feasibility of the recovery.

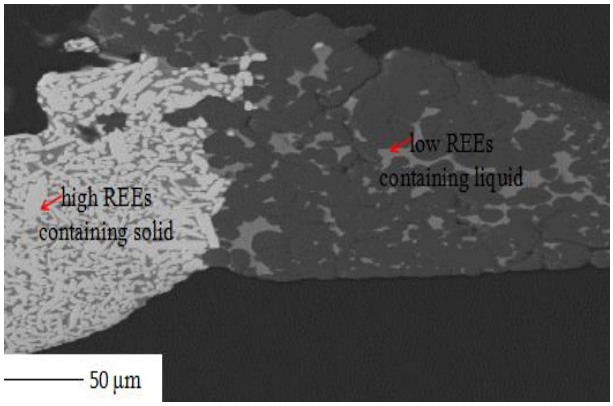

Figure 4: Precipitation of the apatite phase in the liquid slag. The higher density of the Dy_2O_3-rich apatite phase causes this phase to settle to the bottom, leaving a Dy_2O_3 depleted liquid on top.

5. Conclusions

The isothermal sections of the SiO_2-Dy_2O_3-CaO system at 1873 and 1773 K have

been constructed based on experimental results. In particular, the solubility of Dy_2O_3 in the binary phases and in the liquid, as well as the formation of ternary Dy_2O_3-rich phase were determined. From these data, two interesting routes to enhance the recovery of Dy_2O_3 from CaO-SiO_2 based systems were proposed: (1) Slag modification to be in the CS + L region at 1773 K to form upon cooling a Dy_2O_3-enriched liquid phase and Dy_2O_3-depleted CS; (2) Slag modification to be in the ternary SiO_2+$CaDy_4(SiO_4)_3O$+L region and allowing the settlement of the more heavy Dy_2O_3-rich ternary phase in the liquid.

Acknowledgment

We acknowledge the support from National Natural Science Foundation of China under Grant No.51504120 and NSFC-FWO exchange project under Grant No. 5171101430.

References

1. Cheng Xu, Jindrich Kynicky, Martin P. Smith, Antonin Kopriva, Martin Brtnicky, Tomas Urubek, Yueheng Yang, Zheng Zhao, Chen He & Wenlei Song. Origin of heavy rare earth mineralization in South China. NATURE COMMUN., 14598 (2017) 1-7

2. Sander Hoenderdaal, Luis Tercero Espinoza , Frank Marscheider-Weidemann , Wina Graus. Can a dysprosium shortage threaten green energy technologies? Energy, 49 (2013) 344-355

3. Cristian Tunsu, Marino Gergorić. Reclaiming rare earth elements from end-of-life products: A review of the perspectives for urban mining using hydrometallurgical unit operations. Hydrometallurgy,156 (2015) 239-258

4. Ho-Sung Yoon, Chul-Joo Kim, Kyeong-Woo Chung, Sung-Don Kim, Jin-Young Lee, Jyothi Rajesh Kumar. Solvent extraction, separation and recovery of dysprosium (Dy) and neodymium (Nd) from aqueous solutions: Waste recycling strategies for permanent magnet processing. Hydrometallurgy, 165 (2016) 27-43

5. Koen Binnemans, Peter Tom Jones, Bart Blanpain, Tom Van Gerven, Yongxiang Yang, Allan Walton, Matthias Buchert. Recycling of rare earths: a critical review. J. Clean. Prod., 51 (2013) 1-22

6. Nawshad Haque, Anthony Hughes, Seng Limand Chris Vernon. Rare Earth Elements: Overview of Mining, Mineralogy, Uses, Sustainability and Environmental Impact. Resources, 3 (2014) 614-635

7. D. Durinck, F. Engström, S. Arnout, J. Heulens, P. Jones, B. Björkman, B. Blanpain, P. Wollants, Resour. Conserv. Recy., 52 (2008) 1121-1131.

8. EhsanVahidi,FuZhao. Environmental life cycle assessment on the separation of rare earth oxides through solvent extraction. J. Environ. Manage., 203,Part 1 (2017) 255-263

9. MarkL.Strauss, Brajendra Mishra, Gerard P. Martins. Selective Reduction and Separation of Europium from Mixed Rare-Earth Oxides from Waste Fluorescent Lamp Phosphors. Rare Metal Tech., (2017) 31-36

10. Quanyin Tan, Jinhui Li & Xianlai Zeng. Rare Earth Elements Recovery from Waste Fluorescent Lamps: A Review. Critical Reviews in Environmental Science and Technology, 45 (2015) 749-776,

11. Muhamad Firdaus, M. Akbar Rhamdhani, Yvonne Durandet, W. John Rankin, Kathie McGrego. Review of High-Temperature Recovery of Rare Earth (Nd/Dy) from Magnet Waste. J. Sustain. Metall., 2 (2016) 276-295

12. Tobias Elwert, Daniel Goldmann, Thomas Schirmer, Karl S. Affinity of Rare Earth Elements to Silico-Phosphate Phases in the System Al_2O_3-CaO-MgO-P_2O_5-SiO_2, Chemie Ingenieur Technik, 86 (2014) 840-847

13. Alexandra Navrotsky, Wingyee Lee, Aleksandra Mielewczyk-Gryn, Sergey V. Ushakov, Andre Anderko, Haohan Wu, Richard E. Riman. Thermodynamics of solid phases containing rare earth oxides.J. Chem. Thermodynamics 88 (2015) 126-141

14. P.Kofstad, Nonstoichiometry, Diffusion and Electrical Conductivity in Binary Metal Oxide,John Wiley & Sons, New York, (1972) 289

15. Matvei Zinkevich. Thermodynamics of rare earth sesquioxides. Prog. Mater. Sci., 52 (2007) 597-647

16. G. Eriksson, et al. Critical Evaluation and Optimization of the Thermodynamic Properties and Phase Diagrams of the MnO_2-SiO_2 and CaO-SiO_2 Systems. Canadian Metallurgical Quarterly, 1993, 33:13-21

17. L.M. Lopato, Ceramurgia Int. 2 (1978) 18

18. N. A. Toropov, F. Ya. Galakhov, and S. F. Konovalova. INORG. ANAL. CHEM., (1960) 1271-1277

19. M. Hillert, B. Sundman, and Z. Wang: Met. Trans. B, 21B (1990) 303-312

20. H. R. Hoekstra and K. A. Gingerich, Science 146, 1163 (1964)

21. Y.J. Kim and W.M. Kriven. TEM characterization of modulated microstructures in $CaO\text{-}Dy_2O_3$ solid solutions. Ultramicroscopy 37 (1991) 351-361

22.Sung S. Kim, Jun Y. Park, Jun Y. Parka, Thomas H. Sanders Jr.b. Thermodynamic modeling of the miscibility gaps and the metastability in the $R_2O_3\text{-}SiO_2$ systems (R=La, Sm, Dy, and Er). J. Alloys Compds. 321 (2001) 84-90

23. JUN Iro, SILICATE APATITES AND OXYAPATITES, THE AMERICAN MINERALOGIST, 53 (1968) 890-907

24. D.L. Poerschke, T.L. Barth, O. Fabrichnaya, C.G. Levi, Phase equilibria and crystal chemistry in the calcia-silica-yttria system, J. Eur. Ceram. Soc. 36 (2016) 1743-1754

25. David L. Poerschke, Carlos G. Levi. Phase equilibria in the calcia-gadolinia-silica system. J. Alloys Compds. 695 (2017) 1397-1404

26. M. Zhao, L. Song, and X. Fan, The Boundary Theory of Phase Diagrams and Its Application. Springer, Berlin. (2011).

27.Wang G L, Yin C L, Zhao H, et al. Synthesis and conductive properties of the $CaxLa_{10-x}(SiO_4)_6O_{3-x/2}$ oxygen ion conductor. Journal of Harbin Engineering University, 2009, 30 (5):579-583.

References in Table 3

[17] Tang M, Lu P, Valdez J A, et al. Heavy ion irradiation effects in the rare-earth sesquioxide Dy_2O_3. Nuclear Inst & Methods in Physics Research B, 250 (2006) 142-147.

[18] Tang M, Lu P, Valdez J A, et al. The order-disorder phase transformation in ion-irradiated rare earth sesquioxide Dy_2O_3. Physica Status Solidi, 4 (2011) 1171-1174.

[19] Valverde J M, Sanchez-Jimenez P E, Perez-Maqueda L A. Limestone Calcination Nearby Equilibrium: Kinetics, CaO Crystal Structure, Sintering and Reactivity. The Journal of Physical Chemistry C, 119(2015) 1623-1641.

[20] Livia G, et al. Structure and vibrational spectra of crystalline SiO_2 ultra-thin films on Mo (112) Surface Science. 584 (2005) 225-236.

[21] Wright A F, Leadbetter A J. The structures of the β-cristobalite phases of SiO_2 and $AlPO_4$. Philosophical Magazine Series 1, 31 (1975) 11.

[22] Ohashi Y. Polysynthetically-twinned structures of enstatite and wollastonite. Physics & Chemistry of Minerals, 10 (1984) 217-229.

[23] Yang H, Prewitt C T. Crystal structure and compressibility of a two-layer polytype of pseudowollastonite ($CaSiO_3$). American Mineralogist, 84(1999) 1902-1905.

[24] Czaya R. Refinement of the Structure of γ-Ca_2SiO_4. Acta Crystallographica, 27(2010) 848-849

[25] Melzer R, Eberhard E. Phase identification during early and middle hydration of tricalciumsilicate (Ca_3SiO_5). Cement and Concrete Research. 19 (1989) 411-422.

[26] Lv W, Guo N, Jia Y, et al. A potential single-phased emission-tunable silicate phosphor $Ca_3Si_2O_7$: Ce^{3+}, Eu^{2+}, excited by ultraviolet light for white light emitting diodes. Optical Materials. 35 (2013) 1013-1018.

[27] Wang J, Tian S, Li G, et al. Preparation and X-ray characterization of low-temperature phases of R_2SiO_5, (R=rare earth elements). Materials Research Bulletin. 36 (2001) 1855-1861.

[28] Fleet M E, Liu X. Structure and complex twinning of dysprosium disilicate ($Dy_2Si_2O_7$), Type B. Acta Crystallographica. 56 (2010) 940-946.

[29] Nagano T, Kaneko K, Zhan G D, et al. Effect of Atmosphere on Weight Loss in Sintered Silicon Carbide during Heat Treatment. Journal of the American Ceramic Society. 83 (2010) 2781-2787.

[30] Kugimiya K, Steinfink H. Influence of crystal radii and electronegativities on the crystallization of AB2X4 stoichiometries. Inorganic Chemistry. 7 (2002) 385–392.

[31] Millon E, Malaman B, Bonazebi A, et al. Structure cristalline du ferrite hemicalcique $CaFe_4O_7$. Materials Research Bulletin. 21 (1986) 985-994.

[32] Piccinelli F, Speghini A, Mariotto G, et al. Visible luminescence of lanthanide ions in $Ca_3Sc_2Si_3O_{12}$ and $Ca_3Y_2Si_3O_{12}$. Journal of Rare Earths. 27 (2009) 555-559.

[33] Su X, Liu L, Yang Y M, et al. Rare Earth Ions (Ce^{3+}, Eu^{2+} and Eu^{3+}) Activated Silicate Oxyapatites in CaO-Y_2O_3-SiO_2 System for WLEDs. Science of Advanced Materials. 9 (2017) 582-586.